Soft Matter

PAPER

View Article Online
View Journal | View Issue

Cite this: *Soft Matter*, 2023, **19**, 9489

Amphiphilic monomers bridge hydrophobic polymers and water†

Guido L. A. Kusters, ‡[ab] Guogao Zhang, ‡[a] Zheqi Chen [ac] and Zhigang Suo *[a]

Water dissolves a hydrophilic polymer, but not a hydrophobic polymer. Many monomers of hydrophilic polymers, however, are amphiphilic, with a hydrophobic vinyl group for radical polymerization, as well as a hydrophilic group. Consequently, such an amphiphilic monomer may form solutions with both water and hydrophobic polymers. Ternary mixtures of amphiphilic monomer, hydrophobic polymer, and water have recently been used as precursors for interpenetrating polymer networks of hydrophilic polymers and hydrophobic polymers of unusual properties. However, the phase behavior of the ternary mixtures of amphiphilic monomer, hydrophobic polymer, and water themselves has not been studied. Here we mix the amphiphilic monomer acrylic acid, the hydrophobic polymer poly(methyl methacrylate), and water. In the mixture, the hydrophobic polymer can form various morphologies, including solution, micelle, gel, and polymer glass. We interpret these findings by invoking that the hydrophobic and hydrophilic groups of the amphiphilic monomer enable it to function as a bridge. That is, the hydrophobic functional group binds with the hydrophobic polymer, and the hydrophilic functional group binds with water. This picture leads to a simple modification to the Flory–Huggins theory, which agrees well with our experimental data. Amphiphilic monomers offer a rich area for further study for scientific insight, as well as for expanding opportunities to develop materials of self-assembled structures with unusual properties.

Received 27th August 2023,
Accepted 22nd November 2023

DOI: 10.1039/d3sm01129a

rsc.li/soft-matter-journal

Introduction

Living tissues are hybrid materials of dissimilar polymers.[1–3] Mimicking living tissues synthetically faces a challenge: dissimilar polymers normally separate into phases, which are unstable and coarsen in time.[4] Arresting phase coarsening is usually a prerequisite to obtain useful materials. For example, in a previous paper, we have described an interpenetrating network of a hydrophobic polymer and a hydrophilic polymer.[5] We submerge a hydrophobic polymer in a precursor of a hydrophilic polymer, which is an aqueous solution of monomer, initiator, and crosslinker. Although the hydrophobic and hydrophilic polymer do not mix, the hydrophobic polymer imbibes the aqueous precursor. After the monomers polymerize, the hydrophilic polymer and the hydrophobic polymer form an interpenetrating network, which arrests phase separation. We have shown that the interpenetrating network achieves a combination of high water content and high load-bearing capacity simultaneously, which cannot be realized by either the hydrophobic polymer or the hydrophilic polymer individually. The previous paper has studied the mechanical behaviour of the interpenetrating network, but not the mixture of the hydrophobic polymer and the aqueous precursor.

Here, we study the mixture of a hydrophobic polymer and an aqueous precursor of a hydrophilic polymer. The monomer of a hydrophilic polymer is usually amphiphilic, consisting of a hydrophobic vinyl group, –CH═CH_2, and a hydrophilic group. Specifically, in a mixture of the amphiphilic monomer acrylic acid, the hydrophobic polymer poly(methyl methacrylate), and water, we find that the hydrophobic polymer can form various morphologies, including solution, micelle, gel, and polymer glass. We interpret these findings by hypothesizing that the amphiphilic monomer "bridges" the hydrophobic polymer and water. That is, the amphiphilic monomer orients its hydrophobic group to the hydrophobic polymer and its hydrophilic group to water. Our data are not accurately described by the Flory–Huggins theory of mixing, which we attribute to the absence of the "bridging" concept. The bridging concept suggests a simple modification to the Flory–Huggins theory that more accurately captures our data.

Amphiphilic molecules have been used as surfactants to stabilize hydrophobic and hydrophilic polymers in hydro-

[a] *John A. Paulson School of Engineering and Applied Sciences, Harvard University, MA 02138, USA. E-mail: suo@seas.harvard.edu*
[b] *Eindhoven University of Technology, Department of Applied Physics, Eindhoven 5612AZ, The Netherlands*
[c] *College of Chemical and Biological Engineering, Zhejiang University, Hangzhou 310058, China*

† Electronic supplementary information (ESI) available. See DOI: https://doi.org/10.1039/d3sm01129a

‡ These authors contributed to this work equally.

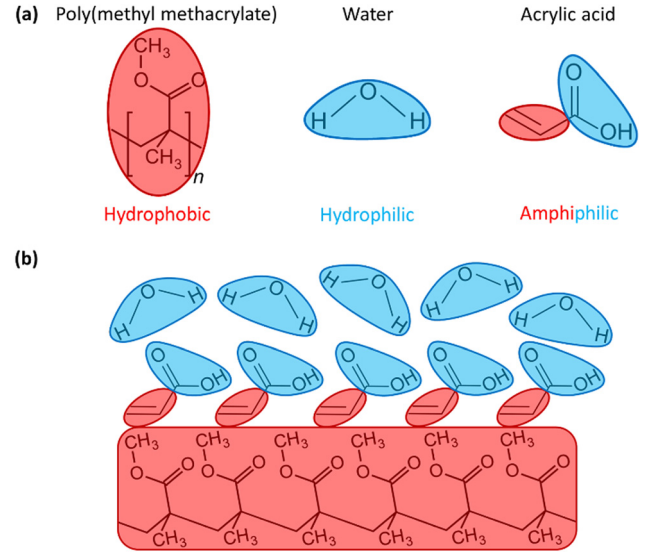

Fig. 1 An amphiphilic molecule bridges a hydrophobic polymer and water. (a) Structures of three molecules: poly(methyl methacrylate) (PMMA) polymer, water, and acrylic acid (AAc) monomer. (b) Amphiphilic AAc bridges hydrophobic PMMA and water.

gels.[6–10] By contrast, mixtures of amphiphilic monomer, hydrophobic polymer, and water have rarely been studied.[5,11] Polymerization of the amphiphilic monomer has been shown to lead to hydrogels of unusual properties.

A mixture of an amphiphilic monomer, hydrophobic polymer, and water

A monomer of a hydrophilic polymer is usually amphiphilic. For example, the monomer acrylic acid (AAc) consists of a hydrophobic vinyl group, –CH═CH_2, and a hydrophilic carboxylic acid group, –COOH (Fig. 1a). AAc and water of any composition can form a solution. The polymer poly(methyl methacrylate) (PMMA) is hydrophobic. In a ternary mixture of AAc, PMMA, and water, the amphiphilic monomer AAc orients its hydrophobic vinyl group to PMMA and its hydrophilic carboxylic acid group to water (Fig. 1b). That is, the amphiphilic monomer ''bridges'' the hydrophobic polymer and water.

The ternary mixture can self-assemble into various structures. When we add PMMA particles of 200 μm diameter into pure water, the PMMA particles remain as a polymer glass (Fig. 2a). We then add different amounts of AAc to the mixture. Some segments of a PMMA chain are decorated by AAc to become mobile in the AAc-water solution, and the remaining segments of the PMMA chain are still immobilized in a glassy domain. When the AAc concentration is low, the glassy domains crosslink the mobile chain segments, and a gel is formed (Fig. 2b). When the AAc concentration is intermediate, the glassy domains no longer crosslink the mobile chain segments, and micelles are formed (Fig. 2c). When the AAc concentration is high, PMMA chains are fully mobile without glassy domains, and a polymer solution is formed (Fig. 2d).

Experimental observations

We prepare a sample as follows. We fill a glass tube with 10 g of water and 0.5 g of PMMA particles. The average diameter of the PMMA particles is 200 μm, and the average molecular weight of PMMA chains is $\sim 35\,000$ g mol^{-1}. We then add various amounts of AAc to the tube, ranging from 0 g to 14 g. To equilibrate samples, we first stir the tubes with a VWR microplate vortex mixer for two days, and then leave them undisturbed for ten days.

We image the samples using a camera. In the absence of AAc, the PMMA-water mixture forms two layers: an opaque sediment at the bottom and a transparent liquid on top (Fig. 3a, top). We extract the bottom layer using a pipette and image it with a microscope (Fig. 3a, bottom). The image shows that the bottom layer consists of the PMMA particles added to the water. The particles do not merge but remain as individual polymer glass particles.

When we add 2 g of AAc to the tube, the mixture separates into an opaque sediment and a transparent liquid (Fig. 3b, top). However, the sediment is thicker than that of the pure PMMA-water mixture, which suggests that PMMA is swollen by the added AAc. The particles still do not merge but remain as individuals (Fig. 3b, bottom).

When we add 4 g of AAc to the tube, the PMMA particles absorb more AAc and merge to form a gel (Fig. 3c, bottom). The gel traps air bubbles and is opaque. The trapped air bubbles

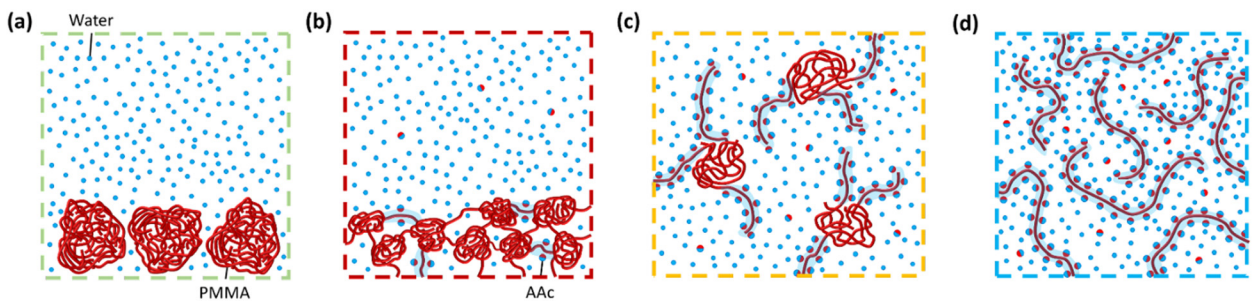

Fig. 2 (a) PMMA glassy particles in pure water. In a ternary mixture of AAc, PMMA and water, PMMA can form (b) a gel, (c) micelles, or (d) a polymer solution.

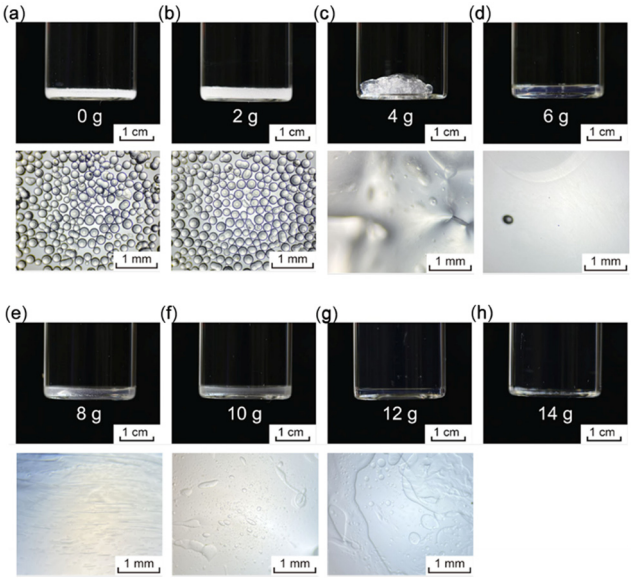

Fig. 3 Experimental observations of PMMA-AAc-water mixtures of various compositions. Tubes are filled with 10 g of water, 0.5 g of PMMA powder, and different amounts of AAc. The equilibrated mixtures are imaged (top). If a mixture separates into two layers, the bottom layer is extracted, put on a glass slide, and imaged with a microscope (bottom). The amount of AAc in each tube is (a) 0 g, (b) 2 g, (c) 4 g, (d) 6 g, (e) 8 g, (f) 10 g, (g) 12 g, and (h) 14 g. In each tube, the height of the solution is 5–7 cm.

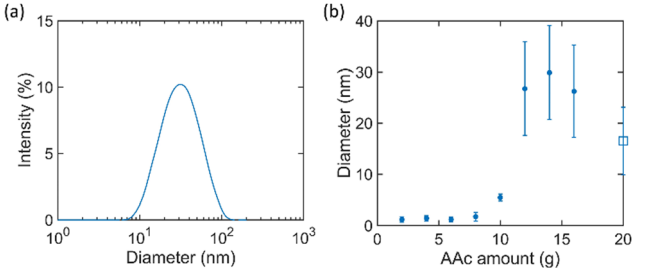

Fig. 4 The size of PMMA-containing microscopic objects in the liquid characterized by dynamic light scattering. (a) The distribution of the hydrodynamic diameter. The amount of AAc in the tube is 11.82 g. The peak is reached when the diameter is 31 nm. (b) The peak of the diameter distribution is plotted as a function of the AAc amount. The error bars indicate the standard deviation. The blue circles represent the liquids in the experiment described in Fig. 3. The open square represents a mixture of 20 g AAc and 0.5 g PMMA.

slowly escape. We can no longer see the individual PMMA particles (Fig. 3c, bottom). When we add 6–12 g of AAc to the tube, the mixture again forms two layers, with less air bubbles in the bottom layer (Fig. 3d–g, top). We likewise cannot distinguish individual PMMA particles (Fig. 3d–g, bottom).

When we add 14 g of AAc to the tube, the PMMA particles are fully dissolved to form a transparent solution (Fig. 3h, top). We do not take a microscopic image of this sample since it does not form two layers.

We interpret the above observations as follows. In the pure PMMA-water mixture, the polymer particles remain as a polymer glass (Fig. 2a). As noted before, when AAc is added to the mixture, some segments of a PMMA chain are decorated by AAc to become mobile in the AAc-water solution, and the remaining segments of the PMMA chain are still immobilized in a glassy domain. When the amount of AAc is 2 g, only a few PMMA chain segments are decorated, and the PMMA particles remain glassy but swell. When the amount of AAc is between 4 g and 12 g, the glassy domains crosslink the mobile chain segments, and a gel is formed. Finally, when the amount of AAc is 14 g or higher, PMMA chains are fully mobile without glassy domains, and a polymer solution is formed.

We characterize the top layer of the mixture with dynamic light scattering (DLS). Some PMMA chains diffuse from the bottom layer to the upper layer. We treat the upper layer as a suspension, where the PMMA molecules undergo Brownian motion in an AAc-water solution. DLS uses fluctuations in the intensity of scattered light to measure the diffusion coefficient of microscopic objects.[12] The Stokes–Einstein equation converts the diffusion coefficient to a hydrodynamic diameter of the microscopic objects. The measurement gives the distribution of the hydrodynamic diameter (Fig. 4a).

The hydrodynamic diameter at the peak of the distribution is plotted as a function of the amount of AAc (Fig. 4b). The error bars give the corresponding standard deviation, and provide a measure for the width of the distribution. In the absence of AAc, pure water dissolves too few PMMA chains to be detected by DLS. For low AAc amounts of 2–8 g, the hydrodynamic diameter is approximately 1–2 nm. For intermediate AAc amounts of 10–16 g, the hydrodynamic diameter goes through a maximum as a function of AAc amount. Finally, for PMMA particles mixed with pure AAc of 20 g, the hydrodynamic radius reaches a value of approximately 17–18 nm (open square in Fig. 4b). For all AAc amounts, the standard deviation is approximately one third of the hydrodynamic diameter at the peak of the distribution. This suggests that adding more AAc to the sample does not increase the polydispersity.

We interpret our findings as follows. For low AAc amounts of 2–8 g, the AAc-water solution is a poor solvent for PMMA molecules. Thus, only a few PMMA molecules escape from the bottom layer to the top layer, and form coils. The volume of a single coiled PMMA chain (v_{PMMA}) can be estimated from the molecular weight of PMMA (35 000 g mol^{-1}), Avogadro's constant, and the density (1.18 g cm^{-3}). The coil size is $\sim v_{PMMA}^{1/3}$ = 3.67 nm, which is comparable to the size obtained from DLS.

For an intermediate AAc amount of 10 g, many PMMA chains are partially decorated by AAc. The partially decorated PMMA chains form micelle-like particles (Fig. 2c). Each micelle particle consists of one or a few PMMA chains, where the undecorated PMMA chain segments form glassy domains, surrounded by decorated (mobile) PMMA chain segments. Some of the micelle particles may even consist of a large number of PMMA chains and multiple glassy domains. These large micelle particles are in effect fragments of a gel, in which multiple glassy domains act as physical crosslinks between decorated, mobile PMMA chains. Some micelle particles diffuse

to the top layer, and others precipitate in the bottom layer. When we shake the tube, the mixture turns opaque as the large micelle particles in the bottom layer mix into the top layer.

At the AAc amount of 12 g, more PMMA chain segments are decorated by AAc. On average the micelle particles are more swollen and larger. Consequently, for the equilibrated sample, the top layer has larger micelle particles than that of the sample prepared with 10 g of AAc, as identified by DLS. In the tube, both layers are transparent, but with different refractive indices. When we shake the tube, the mixture also turns opaque.

For AAc amounts of 14 g and 16 g, the sample forms a homogeneous solution. The hydrodynamic diameter peaks at 14 g, then decreases at 16 g. The diameter maximizes due to a competition between swelling and dissolution of the micelle particles. At a sufficiently large AAc amount, too many PMMA chain segments are decorated by AAc, and individual PMMA chains dissolve in the AAc-water solution.

Finally, in pure AAc the PMMA particles fully dissolve. Since AAc is a good solvent for PMMA, the PMMA molecules have a larger hydrodynamic diameter than individual (coiled) PMMA molecules at low AAc amounts.

Phase behaviour

We plot our experimental observations in a triangle, where each point corresponds to mass fractions of PMMA, AAc, and water added in a tube (Fig. 5). We focus on if the sample forms one or two layers, because we envision applications in which the AAc monomers are polymerized to manufacture materials of unusual mechanical properties. In a recent publication we demonstrated our procedure,[5] for which phase separation is a prerequisite. Each red dot corresponds to a tube in which two layers form (*e.g.*, Fig. 3a–g). This includes the morphologies in Fig. 2a–c. Each blue dot corresponds to a tube in which a single transparent liquid forms (*e.g.*, Fig. 3h). This includes the morphologies in Fig. 2c and d. See the ESI† for more details.

In the lower-left part of the triangle, where the mass fraction of water is large, two layers form in a tube, as the PMMA particles cannot dissolve in an AAc-water solution at these ratios (red dots). In the upper part of the triangle, where the mass fraction of AAc is large, a single liquid forms in a tube, as AAc is a good solvent for PMMA (blue dots). We do not study samples of higher mass fractions of PMMA as the viscosity of the sample is too high to reach equilibrium in a reasonable period of time.

For intermediate AAc-to-water ratios, there exists a transition from tubes in which two layers form to tubes in which a single liquid forms. This transition also depends on the mass fraction of PMMA. Although it is possible to further quantify this transition by measuring the composition of each layer in the tubes (for example, by fluorescent labelling or thermogravimetric analysis),[13] here our aim is to achieve a qualitative understanding of the bridging phenomenon.

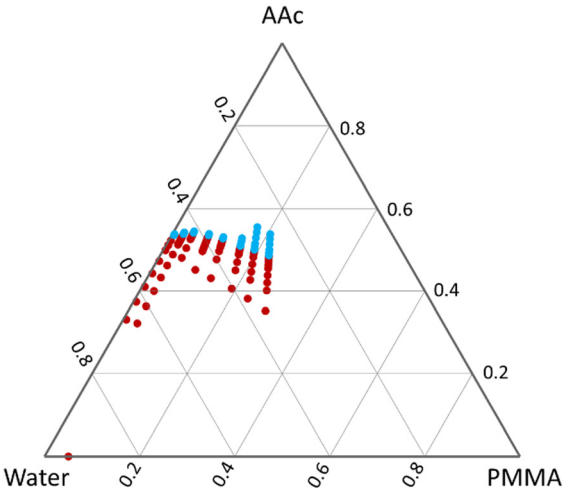

Fig. 5 In a triangle, each point corresponds to the mass fractions of PMMA, AAc, and water added in a tube. The composition in each tube is specified by two numbers: the mass of PMMA divided by the mass of the whole content, and the mass of AAc divided by the mass of the whole content. Each red dot corresponds to a tube in which two layers form. Each blue dot corresponds to a tube in which a single transparent liquid forms.

To better understand the transition, we compare our experimental data with the Flory–Huggins theory of mixing. The free energy density of mixing is[14–18]

$$\begin{aligned}\frac{f(\varphi,\psi)}{k_{\mathrm{B}}T} &= \frac{\varphi}{\nu_{\mathrm{p}}}\log\varphi+\frac{\psi}{\nu_{\mathrm{a}}}\log\psi\\ &+(1-\varphi-\psi)\log|1-\varphi-\psi|\\ &+\chi_{\mathrm{p,a}}\varphi\psi+\chi_{\mathrm{p,w}}\varphi(1-\varphi-\psi)\\ &+\chi_{\mathrm{a,w}}\psi(1-\varphi-\psi).\end{aligned}\tag{1}$$

Here, φ is the volume fraction of PMMA, ψ the volume fraction of AAc, and $1-\varphi-\psi$ the volume fraction of water. Since the densities of PMMA, AAc, and water are similar, for simplicity, we identify these volume fractions with mass fractions when comparing the theory to our experimental data. The first three terms of the free energy density represent the entropy of mixing, with ν_{p} and ν_{a} the volumes of a PMMA molecule and an AAc molecule divided by the volume of a water molecule. The last three terms represent the energy of mixing, with $\chi_{\mathrm{p,a}}$, $\chi_{\mathrm{p,w}}$, and $\chi_{\mathrm{a,w}}$ being the dimensionless measures of the molecular incompatibility between PMMA and AAc, PMMA and water, and AAc and water, respectively.

The free energy density function (1) is a curved surface in the three-dimensional space, with the composition triangle as the horizontal plane, and the free energy density as the vertical axis (Fig. 6a). Each point on the surface represents a homogeneous state. Each point in the triangle represents the composition of the content in a tube. The content in a tube can equilibrate either in a homogeneous state, or in two coexisting homogeneous states. In either case, the state of equilibrium minimizes the total free energy. States of equilibrium are identified by

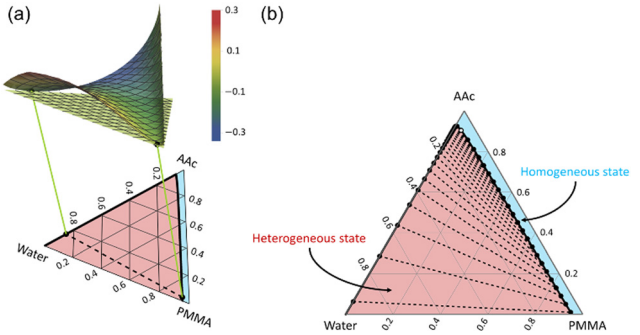

Fig. 6 The Flory–Huggins theory applied to the ternary mixture of PMMA, AAc, and water. (a) The curved surface is the free energy density as a function of composition, which is specified by the mass fractions. The surface is nonconvex, and the magnitude of the free energy density is colour coded. States of equilibrium are identified by planes tangent to the surface. (b) The composition triangle is marked with a region of homogeneous state (blue), a region of coexisting homogeneous states (red), and tie lines (dashed). On the curve demarcating the two regions, black dots represent coexisting homogeneous states, and the white dot represents the critical point. Each tie line connects two coexisting homogeneous states in equilibrium.

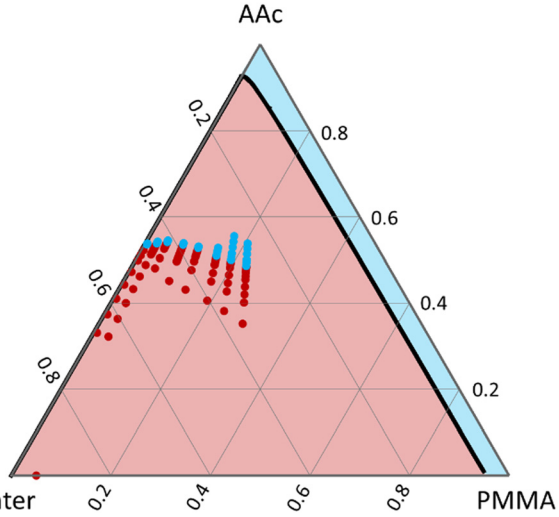

Fig. 7 Comparison of the predictions of the Flory–Huggins theory and experimental data.

planes tangent to the surface. The surface is nonconvex. When a tangent plane touches the surface only at one point and is below the surface, the content in the tube forms a homogeneous state. These compositions are marked in blue in the triangle. When a tangent plane touches the surface at two points and is below the surface, the two points correspond to two coexisting homogeneous states. Connecting the two tangent points is a straight line segment, called a tie line. By the rule of mixture, each point on the tie line corresponds to a mixture of the two coexisting homogeneous states. As the tangent plane rolls under the surface, the sequence of the two tangent points form two curves on the surface. The two curves meet at a point, called the critical point. The tie line is projected onto the composition triangle as a dashed line segment. Also marked in the composition triangle as a black curve is the sequence of coexisting homogeneous states. The compositions marked in red are enclosed by the black curve, and so each lie on a tie line. The homogeneous state is thus thermodynamically unstable for the compositions in red, which instead separate into a mixture of two coexisting homogeneous states in equilibrium. The coexisting states are indicated by the two ends of the tie line.

In Fig. 6b, the composition triangle is marked with a region of homogeneous state of equilibrium, a region of heterogeneous state of equilibrium, and tie lines. As the mass fraction of AAc increases, the tie lines shorten, and collapse into a point, the critical point. The critical point lies close to the left edge of the composition triangle, corresponding to a low mass fraction of PMMA, because the molecular weight of the PMMA molecules ($\sim$35 000 g mol^{-1}) far exceeds those of AAc and water (72.06 g mol^{-1} and 18.02 g mol^{-1}, respectively). Inspecting the free energy density of mixing (1), we note that the long PMMA molecules negligibly contribute to the entropy of mixing. As a result, even small amounts of PMMA do not readily dissolve in the mixture, unless there is an energetic incentive to do so. That is, unless the AAc amount is sufficiently high.

We next compare the prediction of the Flory–Huggins theory to our experimental data (Fig. 7). The theory predicts that the mixture forms two layers if the water fraction is moderate to high, and that the mixture forms a homogenous state if the water fraction is low. Our data is in line with these qualitative trends, and confirms that even small amounts of AAc do not dissolve in the mixture below a critical amount of AAc. However, the theory overestimates the amount of AAc required to dissolve PMMA in the ternary mixture.

To plot Fig. 7, we need values of the three interaction parameters, $\chi_{p,w}$, $\chi_{a,w}$, and $\chi_{p,a}$. The first is available in the literature,[19] $\chi_{p,w}$ = 2.34. Although no data is available for the interaction parameter between acrylic acid and water, the interaction parameter between poly(acrylic acid) and water is known.[20] We assume that the two have similar values, $\chi_{a,w}$ = 0.41. No value of $\chi_{p,a}$ is available in the literature. Anticipating that the theory will overestimate the AAc amount required to dissolve PMMA in the ternary mixture, we set $\chi_{p,a}$ = 0. This value is the lower bound for $\chi_{p,a}$, since negative values would imply a mutual attraction between PMMA and AAc.[21] We use this lower bound because increasing $\chi_{p,a}$ further suppresses the formation of a homogeneous state, and so worsens the prediction.

Efforts have been made to modify the Flory–Huggins theory to better fit experimental data. For example, a ternary interaction parameter, χ_T, has been introduced to account for three-body interactions.[22,23] Alternatively, one (or more) of the interaction parameters have been fitted as a function of composition.[24]

Here we appeal to the concept that the amphiphilic molecule AAc bridges the hydrophobic polymer PMMA and water. The original Flory–Huggins theory disregards the amphiphilic nature of the AAc molecules. In the theory, if an AAc molecule comes in contact with PMMA or water, the same interaction

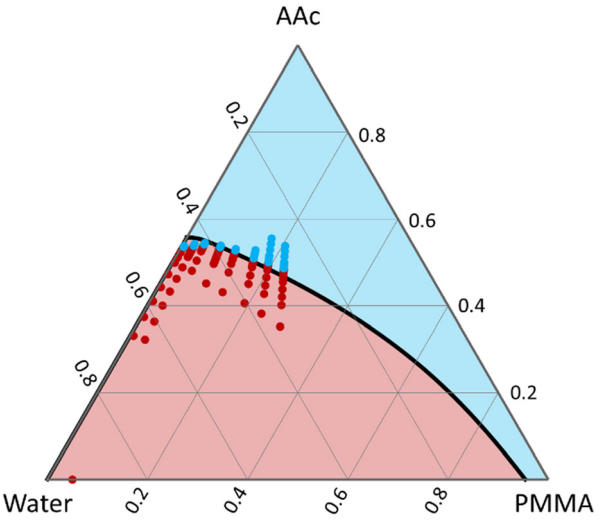

Fig. 8 Flory–Huggins theory modified with a three-body term, corresponding to the concept that the amphiphilic molecule AAc bridges the hydrophobic polymer PMMA and water.

energy $\chi_{p,a}$ or $\chi_{a,w}$ applies, regardless of the orientation of the AAc molecule. That is, any time an AAc molecule bridges PMMA and water, the theory overestimates the cost of energy. After all, for a bridging AAc molecule, only the hydrophobic functional group interacts with PMMA and only the hydrophilic functional group interacts with water.

To correct for this overestimate in the original Flory–Huggins theory, we superimpose to the free-energy density a three-body term:

$$-k_B T g_{\text{bridge}} \varphi\psi(1-\varphi-\psi) \qquad (2)$$

The negative sign indicates that the amphiphilic bridging lowers the free energy of mixing, and the product $\varphi\psi(1-\varphi-\psi)$ indicates that all three components – AAc, PMMA, and water – are required for bridging. This correction (2) can be interpreted as effectively lowering the interaction energy between PMMA and water in the presence of AAc. Furthermore, it is the lowest-order correction involving all three components that is admissible by symmetry.

Using $g_{\text{bridge}} = 2.09$ as a fitting parameter, we re-calculate the theoretical phase diagram. The amphiphilic bridging markedly lowers the energy of mixing, and greatly enlarges the region of homogenous solution (Fig. 8). The critical point moves lower in the composition triangle. The experimental data and the modified theory agree well. The theory can be used to predict the range of compositions that result in two-layer samples, which can be used to achieve materials of unusual properties. The theory also predicts the water content in each layer, which we have shown in a recent publication to have a significant effect on the mechanical properties of the material.[5]

To further test the notion of amphiphilic bridging, we mix the methyl methacrylate (MMA) monomer with AAc and water. Compared to the PMMA polymer, the MMA monomer increases the entropy of mixing. Consequently, the original Flory–Huggins theory predicts a lower critical point for the MMA-AAc-water mixture than for the PMMA-AAc-water mixture (Fig. 9a). However, our experimental data indicates an even lower critical point. After we introduce the same three-body term (2), with the same fitting parameter value, $g_{\text{bridge}} = 2.09$, the modified theory does lower the critical point to a position comparable to the experimental data (Fig. 9b). The theoretical prediction and experimental data can of course be further matched if we adjust values of fitting parameters or add new terms. Because the experimental data and the theory modified with a three-body term are already close, we have decided not to modify the theory any further.

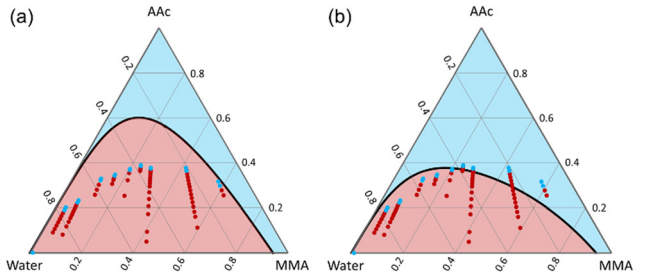

Fig. 9 Theoretical predictions and experimental data for MMA-AAc-water ternary mixtures. (a) Original Flory–Huggins theory. (b) Flory–Huggins theory modified with a three-body term, eqn (2).

Conclusion

We have shown that an amphiphilic monomer can bridge a hydrophobic polymer and water, forming homogeneous ternary solutions for a large range of compositions. Here we mix the amphiphilic monomer acrylic acid, the hydrophobic polymer poly(methyl methacrylate), and water. In the mixture, the hydrophobic polymer can form various morphologies, including solution, micelle, gel, and polymer glass. We interpret these findings by invoking that the amphiphilic monomer has both hydrophobic and hydrophilic functional groups. The former binds with the hydrophobic polymers, and the latter binds to water. This amphiphilic bridging is missing in the original Flory–Huggins theory of mixing. We modify the original Flory–Huggins theory by adding a three-body interaction term, with a single fitting parameter. The modified Flory–Huggins theory agrees with the experimental data well. As demonstrated in our previous paper,[5] the mixtures of diverse morphologies can serve as precursors for hydrogels of unusual properties.

Materials and methods

Materials

Poly(methyl methacrylate) (178765000, average molecular weight $\sim$35 000 g mol^{-1}) was purchased from Thermo Scientific. Acrylic acid (147230-500G) was purchased from Sigma-Aldrich. Deionized water was purchased from Poland Spring. All the chemicals were used as received.

Dynamic light scattering (DLS)

All DLS tests were conducted at 298 K using a Zetasizer Nano ZS machine. Zetasizer Software (Version 7.13) was used to analyze the data. The input included the test temperature and the viscosity of the solvent. At 298 K, water has a viscosity of $\sim$ 0.0089 poise, and acrylic acid has a viscosity of $\sim$ 0.0120 poise.[25] Because of the minor difference in viscosity and to simplify the analysis, the viscosity of water is used for all the DLS analyses.

Fitting procedure

As input for the fitting procedure we use the experimental data points in each series of measurements that are closest to the phase boundary. If the data points on either side of the boundary (red and blue) are sufficiently close to each other, we can estimate the experimental phase boundary by taking their average. The fitting then proceeds by performing the Flory–Huggins binodal calculations for various values of g_{bridge} (we loop over this parameter), and computing the shortest distance of each estimated phase boundary data point to the theoretical curve. We measure this distance in the composition triangle using the independent coordinates φ and ψ. The fitting procedure minimizes the squared distance, summed over all estimated phase boundary data points: $\sum_{i\in\mathrm{data}} \left(\Delta\varphi_i^2 + \Delta\psi_i^2\right)$.

Conflicts of interest

There are no conflicts to declare.

Acknowledgements

This work was supported by Harvard University MRSEC (DMR-2011754) and by the Air Force Office of Scientific Research (FA9550-20-1-0397). G. L. A. K. acknowledges funding from the Dutch Research Council (NWO) in the framework of the ENW PPP Fund for the top sectors and from the Ministry of Economic Affairs in the framework of the 'PPS-Toeslagregeling'. Z. C. acknowledges funding from the Academic Rising Star Program for PhD students in Zhejiang University.

References

1 E. A. Lumpkin and M. J. Caterina, *Nature*, 2007, **445**, 858–865.
2 S. V. Murphy and A. Atala, *Nat. Biotechnol.*, 2014, **32**, 773–785.
3 L. Zhang, L. Fu, X. Zhang, L. Chen, Q. Cai and X. Yang, *Biomater. Sci.*, 2021, **9**, 1547–1573.
4 M. Rubinstein and R. H. Colby, *Polymer Physics*, 2003.
5 G. Zhang, J. Kim, S. Hassan and Z. Suo, *PNAS*, 2022, **119**, e2203962119.
6 C. H. Lee and Y. C. Bae, *RSC Adv.*, 2016, **6**, 103811.
7 Q. Zhang, M. Wu, X. Hu, W. Lu, M. Wang, T. Li and Y. Zhao, *Macromol. Chem. Phys.*, 2019, **221**, 1900320.
8 C. N. Zhu, S. Y. Zheng, H. N. Qiu, C. Du, M. Du, Z. L. Wu and Q. Zheng, *Macromolecules*, 2021, **54**, 8052–8066.
9 D. Das, E. Cha, S. Lee, H. Shin and I. Noh, *Biomacromolecules*, 2022, **21**, 892–902.
10 C. Seyrig, A. Poirier, J. Perez, T. Bizien and N. Baccile, *Biomacromolecules*, 2023, **24**, 19–32.
11 G. Zhang, J. Steck, J. Kim, C. H. Ahn and Z. Suo, *Sci. Adv.*, 2023, **9**, eadh7742.
12 B. J. Berne and R. Pecora, *Dynamic Light Scattering: With Applications to Chemistry, Biology, and Physics*, John Wiley & Sons, 1976.
13 Y. Luo, M. Gu, C. E. Edwards, M. T. Valentine and M. E. Helgeson, *Soft Matter*, 2022, **18**, 3063–3075.
14 M. L. Huggins, *J. Phys. Chem.*, 1942, **46**, 151–158.
15 M. L. Huggins, *J. Am. Chem. Soc.*, 1942, **64**, 1712–1719.
16 P. J. Flory, *J. Chem. Phys.*, 1942, **10**, 51–61.
17 P. J. Flory and W. R. Krigbaum, *Annu. Rev. Phys. Chem.*, 1951, **2**, 383–402.
18 H. Tompa, *Polymer Solutions*, Academic Press, New York, 1956.
19 J.-Y. Lai, S.-F. Lin, F.-C. Lin and D.-M. Wang, *J. Polym. Sci. Pol. Phys.*, 1998, **36**, 607–615.
20 A. P. Safronov, L. V. Adamova, A. S. Blokhina, I. A. Kamalov and P. A. Shabadrov, *Polym. Sci., Ser. A*, 2015, **57**, 33–42.
21 P. J. Flory, *Discuss. Faraday Soc.*, 1970, **49**, 7–29.
22 B. E. Read, *Trans. Faraday Soc.*, 1960, **56**, 382–390.
23 J. Pouchlý, A. Živný and K. Šolc, *J. Polym. Sci. Pol. Sym.*, 1968, **23**, 245–256.
24 F. W. Altena and C. A. Smolders, *Macromolecules*, 1982, **15**, 1491–1497.
25 K. F. Fazende, D. P. Gary, J. D. Mota-Morales and J. A. Pojman, *Macromol. Chem. Phys.*, 2020, **221**, 1900511.